



Report No: 25272/1/16

Date: July 2016

For: Department for Transport

A large blue graphic with a world map background, featuring a grid of latitude and longitude lines. The graphic is composed of several overlapping rectangular shapes in various shades of blue, creating a layered effect.

**Department for Transport Technical Assessment of
Petroleum Tankers: Assessment of BS EN 13094 Lap and
Partition Joint Designs**

TWI Ltd

TWI is one of the world's foremost independent research and technology organisations, with expertise in solving problems in all aspects of manufacturing, fabrication and whole-life integrity management technologies.

Established at Abington, Cambridge, UK in 1946 and with facilities across the globe, the company has a first-class reputation for service through its teams of internationally respected consultants, scientists, engineers and support staff. The company employs over 900 staff, serving over 700 Member companies across 4500 sites in 80 countries.

TWI is a non-profit distributing company, limited by guarantee and owned by its Members. It can therefore offer confidential, independent advice and is internationally renowned for employing multidisciplinary teams to implement established or advanced joining technology or to address issues associated with initial design, materials selection, production and quality assurance, through to service performance and repair.

Supported by a successful international training and examinations network, TWI also takes technical and practical knowhow to regions looking for growth through skills development.

TWI houses the National Structural Integrity Research Centre for postgraduate education, and a professional institution, The Welding Institute, which has a separate membership of over 6000 individuals.

The company operates a management system certificated by LRQA to BS EN ISO 9001:2008. It also has certificated management systems for health and safety (BS OHSAS 18001) and environment (BS EN ISO 14001).

(See inside back cover TWI Management System.)

TWI Report: Department for Transport Technical Assessment of Petroleum Tankers: Assessment of BS EN 13094 Lap and Partition Joint Designs

Report No: 25272/1/16

Date: July 2016


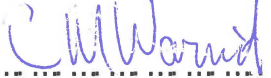
Prepared for: **Department for Transport**
c/o Zone 2/31
Great Minster House
33 Horseferry Road
London
SW1P 4DR

Contact: Steve Gillingham

Authors: Tyler London and Simon Smith

TWI Endorsement

This report has been reviewed in accordance with TWI Policy

Project Leader...  .. Technical Reviewer...  ..
(Signature) (Signature)

Print name: Tyler London

Print name: Marcus Warwick

Administrator...  ..
(Signature)

Print name: Caroline Knight

Published Version History

Date	Version	Reason
25/11/2015	0.1	Draft issue to DfT for comments
06/01/2016	0.2	Draft issue incorporating comments and appendix
08/01/2016	0.3	Draft issue of Appendix B
01/07/2016	0.4	Incorporation of comments from 19 May 16

Contents

1	Introduction	1
2	Background	1
3	Objective	3
4	Finite Element Analysis	3
4.1	Software	3
4.2	Geometry	3
4.3	Finite element mesh	4
4.4	Material properties	4
4.5	Loads and boundary conditions	5
4.6	Results and discussion	5
5	Conclusions	6
6	Discussion of Further Work	6
7	Recommendations	7
8	References	8

Figures 1-8

Appendix A: Dimensions for the End Joint Design Geometries

**Appendix B: Numerical Assessment of End Joint Designs Under Topple
Test Conditions**

1 Introduction

Following the Department for Transport (DfT) acceptance of TWI Ltd (TWI) Proposal PR23024-2 (TWI, 2014) as part of the DfT technical assessment of petroleum tankers, TWI has been requested to supply additional Work Package 2 extensions to supplement the original work and project management activities. In relation to sub-sections of the DfT research specification (DfT, 2014), the proposal for this additional work, TWI Proposal PR25351-3 (2015a), is concerned with the Work Package 2 extension activities related to:

- Engaging in further peer review activities including project meetings and dissemination of findings (Section 5.2, Requirement 2.9);
- Assessing existing/proposed non-destructive inspection methods to determine whether such methods would be an effective and viable means of checking conformity and condition of tankers at initial and subsequent inspections (Section 5.2, Requirement 2.12);
- Extending modelling and ECA to analyse safety of GRW tankers under representative rollover and collision loads based on relevant impact conditions, taking into account data collected in WP2 and WP3. (Section 5.2, Requirement 2.13);
- Extending modelling and ECA to include modified and/or compliant tankers (in addition to non-compliant tankers) and determine relative level of safety and fatigue life in comparison with that required by ADR, including, as appropriate, metallographic examination of sections from said tankers and mechanical tests of samples taken from those sections so as to determine, amongst other things, characteristics of circumferential welds and any flaws identified therein (Section 5.2, Requirement 2.14);
- Assessing the feasibility and cost of proposed modification(s) and associated procedure(s) of tanker design and construction (Section 5.2, Requirement 2.15);
- Undertaking non-destructive examination, destructive examination, destructive testing, modelling and of various other aspects of tanker construction to compare tankers and check for compliance (Section 5.2, Requirement 2.16).

This report addresses the following task in relation to the above activities:

- Numerical assessment of informative joint designs as per BS EN 13094 (2015) for petrol tanker lap and partition joints under topple test conditions.

2 Background

The present report concerns the numerical assessment of the propensity for petroleum road fuel tanker end joints made in accordance with Annex D of BS EN 13094:2015 (or with respect to a previous version of 13094, depending on the date of the design and manufacture of the specific tanker analysed) to rupture under topple test conditions by applying a forming limit diagram methodology. Previous reports issued within the DfT research programme on the assessment of the structural integrity of petroleum road fuel tankers (TWI, 2015a-b) analysed manufacturer-specific joint designs, including the rear end dishes of tankers herein described as 'Actual Banded Type 1' and 'Actual Banded Type 2'.

Initially, the analysis of Actual Banded Type 1 (TWI, 2015b) was undertaken to provide a mechanistic explanation for the ruptures that were observed in the end dish metal at the ends of the flattened extent of the rear end dish after the topple test (see Figure 1). Using the following information, the forming limit

diagram and associated finite element simulations provided an explanation, based on established physical principles and modelling techniques, for the observed ruptures:

- A lower-bound forming limit curve obtained from a brief literature review for aluminium alloy EN AW-5182 (also referred to as AA 5182-O in other DfT technical assessment of petroleum tanker reports);
- A simplified representation of the Actual Banded Type 1 rear end joint geometry;
- Isotropic and homogeneous tensile properties measured from samples taken from the weld metal and tanker shell of Actual Banded Type 1 that were representative of EN AW-5182 (AA 5182-O);
- A static idealisation of the topple test loading conditions.

Based on the success of the method in predicting the experimentally-observed ruptures in Actual Banded Type 1, the method was then applied to tanker Actual Banded Type 2 to see if it would predict the absence of ruptures observed in the rear end dish of this tanker after topple testing. The same finite element modelling approach was employed, except that:

1. The precise geometry was modelled, based upon engineering drawings provided by the manufacturer, and measurements taken from the tanker itself.
2. The lower bound, experimentally-measured tensile properties of the tanker shell were assigned to the end dish, tanker shell and weld metal regions, whilst the as-measured tensile properties of the extrusion band (typically higher strength than the tanker shell) was assigned to the extrusion band region in the model.

In this case, analysis of the strain field in the vicinity of the end dish to extrusion band joint did not identify any locations that exceeded the previously-identified, lower-bound, EN AW-5182 (AA 5182-O) forming limit curve (ie no points in the model exceeded the formability limit of the material). In other words, the same method that predicted ruptures for Actual Banded Type 1, did not predict ruptures for Actual Banded Type 2. Furthermore, the in-plane deformation of the extrusion band to end dish joint in the finite element model was compared with macrographs prepared from samples taken from the crushed side of Actual Banded Type 2, and the agreement was seen to be very strong and further validated the finite element modelling methodology.

Although some assumptions made in the finite element simulations and the subsequent assessment of the numerical results may have been inconsistent with the actual full-scale test (such as the material property definitions and geometric idealisations), the finite element modelling methodology was able to provide an engineering explanation for the appearance of the observed ruptures. The predictions from these two studies where full-scale topple test experimental measurements were available therefore provided confidence that the forming limit diagram methodology could possibly be used to predict the likelihood for ruptures to occur under topple test conditions for any petroleum road fuel tanker end joint design similar to Actual Banded Type 1 and Actual Banded Type 2. More specifically, it was hypothesised that the forming limit diagram method could be used to assess and quantitatively compare (subject to the same assumptions made in the previous analyses) the informative joint designs in Annex D of BS EN 13094, specifically those illustrated in D.14(a-c) and D.7(a-b).

3 Objective

In light of the previous analyses, the objective of the present study is to analyse the informative joint designs in Annex D of BS EN 13094 under topple test conditions and to assess the results using the previously validated forming limit diagram methodology.

4 Finite Element Analysis

4.1 Software

All models were generated using the commercial finite element analysis software suite Abaqus (SIMULIA, 2014). The models were developed in Abaqus/CAE v6.14-2, analysed using the static solver, Abaqus/Standard, and post-processed with Abaqus/Viewer.

4.2 Geometry

Three different joint designs were developed and analysed as follows:

- **Generic Banded Type 1.** This joint design was developed from Figure D.14(a) of BS EN 13094 (reproduced in Figure 2) and is qualitatively similar to the rear end dish of the Actual Banded Type 1 design that is shown in Figure 3;
- **Generic Banded Type 2.** This joint design was developed from Figures D.14(b-c) of BS EN 13094 (also reproduced in Figure 2) and is qualitatively similar to the rear end dish of the Actual Banded Type 2 design obtained from a manufacturer's engineering drawings;
- **Generic Stuffed Design.** This joint design was developed from Figures D.7(a-b) (reproduced in Figure 4) and is qualitatively similar to the rear end dish of the proof-of-concept tanker (HSL, 2014).

Whilst there are some enforced relationships between the various geometric dimensions of the constituent parts of the joint designs in Annex D, the designs are not fully-constrained in the sense that there is significant freedom in actually defining a joint design that is consistent with the guidelines in Annex D. First, in an attempt to make the finite element models representative of the illustrations in Annex D, the illustrations of the joint designs were 'scaled' with respect to known dimensions, such as the 5mm tanker shell thickness. However, this was found to be ill-advised for certain aspects of the end joint designs (moreover, there is nothing stated in the standard that indicates the designs are drawn to scale). Therefore to ensure that the analyses were conducted in a manner that was consistent with existing tanker designs, TWI compiled the relevant dimensional inequalities and recommended a series of specific dimensions to be used within the present study. This list was circulated to DfT and, following peer review by DfT and other third parties, the dimensions described in Appendix A of this report were used to define all aspects of the finite element model geometry. Images of the geometries of the finite element models are shown in Figure 5.

Quarter symmetry has been employed and a Cartesian coordinate system is shown in the top left of this figure. To provide an orientation of the finite element model with respect to position of the tank in the topple test, an illustration of the topple test has been provided at the top of Figure 5. The (y,z)-plane in the model corresponds to the BD symmetry plane in the diagram; the (x,z)-plane in the model corresponds to the AC symmetry plane in the diagram. This is discussed further in Section 4.5.

4.3 Finite element mesh

The finite element mesh was comprised of two distinct regions: the local region including the tanker shell, extrusion band (when present) and outer rim of the end dish adjacent to the extrusion band was modelled with solid, continuum elements, and the remainder of the end dish was modelled with shell elements. Because the model involved large deformations, nonlinear material response and nonlinear contact, linear, reduced-integration, hexahedral elements (type C3D8R) were used in all solid regions to improve convergence, as quadratic-displacement elements (such as C3D20R) are not well-suited for contact problems and problems involving significant mesh deformation. To ensure the accuracy of the mesh comprised of linear elements, a suitable mesh sensitivity study was undertaken to determine a mesh density that resulted in converged strains in the area of interest. The shell element region of the end dish was comprised of quadratic shell elements (type S8R in Abaqus) and the incompatible interface between the shell and solid elements was joined by a shell-to-solid coupling in Abaqus. This coupling ensures that the rotational degrees of freedom of the shell element nodes are appropriately interpolated and constrained with the solid element nodes along the incompatible interface. The best practice rules detailed in the Abaqus Analysis Manual that are associated with this kind of coupling were implemented in the model. Images of the finite element meshes for Generic Banded Types 1 and 2 are shown in Figure 6.

4.4 Material properties

As described in Section 2, the previous Actual Banded Type 1 model contained a single, isotropic, homogeneous material, whilst the Actual Banded Type 2 model contained two distinct materials: one for the extrusion band and one for the tanker shell, weld metal and end dish. In order to provide consistency with these previous analyses, whilst not using the specific, experimentally-measured tensile properties from previous research work, idealised stress-strain curves were employed for the present work. Two materials were defined:

- **Material A** was defined to be similar to the generic tensile properties of EN AW-5182 (AA 5182-O):

□ Young's modulus:	70GPa
□ Yield stress (0.2% proof strength):	130MPa
□ Ultimate tensile strength:	275MPa
□ Elongation:	21%

- **Material B** was defined to have elevated tensile properties and reduced elongation capacity compared with EN AW-5182 (AA 5182-O):

□ Young's modulus:	70GPa
□ Yield stress (0.2% proof strength):	350MPa
□ Ultimate tensile strength:	400MPa
□ Elongation:	7%

The tensile properties specified above were used to construct a Ramberg-Osgood stress-strain curve that exhibited continuous yielding (see Figure 7). This stress-strain curve was then appropriately converted to true stress and true plastic strain and used in the finite element models.

For each geometry, two separate finite element models were analysed: one with all regions behaving as Material A, and one with the tanker shell, weld metal and end dish comprised of Material A, whilst the extrusion band was comprised of Material B. This approach allowed for the effect of different

materials to be considered for the joint designs similar to Actual Banded Type 1 (ie Generic Banded Type 1 joints). The Generic Stuffed Design joint did not contain an extrusion band, and therefore only one analysis was undertaken, assuming the entire modelled region to be comprised of Material A.

4.5 Loads and boundary conditions

As detailed in the previous forming limit diagram assessment reports (TWI, 2015a-b), the ground was modelled as a flat, rigid, analytic surface that was coupled to a centrally-positioned reference node. This reference node was statically displaced in the x-direction, resulting in the ground pressing against the side of the tanker. All other translational and rotational degrees of freedom of this reference node were restrained. As only one quarter of the tanker was modelled, the symmetry plane opposite the ground was restrained in the x-direction, resulting in the tanker deforming ('crushing') in response to the ground movement. The other symmetry plane (ie that representing symmetry plane AC of the tank in Figure 5) was restrained in the y-direction. Finally, the free surface of the extruded length of tanker shell was restrained in the longitudinal (z-) direction.

All finite element models were analysed under the finite strain assumption so that the nonlinear effect of large displacements and rotations was incorporated into the analysis (ie the NLGEOM option in Abaqus was activated).

Because the global stiffness (or compliance) of each geometry was different, the total force required to displace the ground a fixed total amount was different for each model. All models were subjected to a 300mm ground displacement, but the simulations were not all assessed at a solution increment corresponding to the same ground displacement. Instead, an alternative method, discussed in Section 4.6 was employed to provide a consistent interpretation of the results of the simulations.

4.6 Results and discussion

In the previous analyses of Actual Banded Type 1 and Actual Banded Type 2, the ground displacement was increased until the resultant flattened length of the tanker matched that which was measured experimentally. However, as the present analyses focussed on idealised joint geometries that were not associated with any specific manufacturer design or experimental topple test data, it was not possible to use this method for determining the solution increment at which to assess the strains against the forming limit curve.

Instead, for each finite element model, the Abaqus output variable 'ALLWK', which is the external work, was monitored as a function of the applied ground displacement. ALLWK, in the case of these simulations, is the work done by the ground on the tanker, which is equal to the sum of the energy dissipated through plastic deformation (plastic dissipation), the total (elastic) strain energy, and the energy dissipated through frictional contact and sliding. The previous simulations of Actual Banded Type 1 and Actual Banded Type 2 were re-visited to determine if the total energy dissipation was similar, even though both simulations required different applied 'crushing' displacement. It was observed that the energy dissipation levels agreed to within 8%. It was therefore decided to use the average value of energy dissipation, approximately $8.5 \times 10^6 \text{N.mm}$, from the Actual Banded Type 1 and Actual Banded Type 2 simulations for the assessments of the joint designs within the present study.

To that end, for each simulation, the solution increment at which the ALLWK variable was closest to the target energy dissipation value was first identified.

At this solution increment, a circumferentially-oriented path of nodes was created along the inner surface of the end dish, just above the weld joining the end dish to the extrusion band. The precise location of this path was selected by identifying where in this region the principal strains were largest, and in particular, the apex of the localised bending deformation. At each node in this path, the maximum and minimum principal strains were output. The results were then plotted on the forming limit diagram as previously described in the TWI reports (2015a-b). The results are shown in Figure 8. A second sensitivity check was undertaken to ensure that the strain plots in the forming limit diagram were not overly sensitive to the solution increment selected (as not all simulations had a solution increment at which the total work variable identically equalled the target level of energy dissipation). It was observed that the strains were not sensitive.

5 Conclusions

From the forming limit diagram shown in Figure 8, the following conclusions can be made:

1. The three curves that exceed the forming limit curve are those corresponding to Actual Banded Type 1 and the Generic Banded Type 1 models (both 1- and 2-material simulations).
2. The Actual Banded Type 2 and Generic Banded Type 2 models (both 1- and 2-material simulations) all fall below the forming limit curve. The curves associated with the models generated from the diagrams in BS EN 13094 (ie the purple and green curves) are closer to exceeding the forming limit curve than that corresponding to Actual Banded Type 2.
3. The curve for the Generic Stuffed Design is far below the forming limit curve. Comparison of the deformation of the tanker in the Generic Stuffed Design simulation with the proof-of-concept tanker showed less agreement than the banded design simulations showed with their corresponding full scale tests. This is likely due to the overloading of the proof-of-concept tanker, but also may indicate that a different approach might be required for the stuffed design analyses.

To provide an estimate of the effect of changing the forming limit curve by a small amount, error bars corresponding to +/- 2% strain have been added.

6 Discussion of Further Work

Although the forming limit curve employed in the present and previous studies was obtained from a brief literature review, and therefore has limitations for wider use due to the known dependency of the curve on strain-rate, test temperature and specimen thickness, the use of formability limits is well-established in other codes and standards. For example, when assessing the acceptability of a corrosion defect or a region of local metal loss in pressure equipment, the American Petroleum Institute standard API-579/ASME FFS (API, 2007; Seipp, 2013) can be used. In API-579, Annex B gives guidance on the use of non-linear, elastic-plastic finite element analysis similar to that used in this report. To assess whether or not a given defect will fail by local plastic collapse (or 'local failure'), the analyst is required to identify a position within the corroded region that exhibits high levels of equivalent plastic strain, ϵ_{peqr} , when the pressure equipment is subjected to the most severe load case. At this location and under the worst-case loading conditions, the analyst must then output the three principal stresses, σ_1 , σ_2 , and σ_3 , and calculate the corresponding equivalent (or Von Mises) stress, σ_e . The analyst then uses the look-up table B1.6 to obtain (or calculate) material-specific parameters α_{sl} , ϵ_{Lu} and m_2 depending on whether the component under consideration is comprised

of a ferritic steel, stainless steel, aluminium alloy or other types of materials. The stresses determined from the finite element model are then combined with the material-specific parameters and input into Equation B1.6 to calculate the limiting triaxial strain:

$$\varepsilon_L = \varepsilon_{Lu} \cdot \exp \left[- \left(\frac{\alpha_{sl}}{1+m_2} \right) \left(\left\{ \frac{(\sigma_1 + \sigma_2 + \sigma_3)}{3\sigma_e} \right\} - \frac{1}{3} \right) \right]$$

The equivalent plastic strain is then compared with this limiting triaxial strain. If ε_{peq} is less than ε_L , then the corrosion defect is deemed to be acceptable and will not fail by local plastic collapse; if ε_{peq} is greater than or equal to the limiting triaxial strain, then the defect is not acceptable and may lead to failure.

Further inspection of the method described above, shows that it is essentially a three-dimensional representation of the forming limit diagram approach: the strain state at a point in the deformed body is compared with a limiting value to determine if failure is likely to occur. The limiting strain value, like in the two-dimensional forming limit diagram, depends on the level of local biaxiality or triaxiality. It may therefore be possible to use this approach to re-assess the simulations undertaken to date. The benefit would be that these revised assessments would not be based on a forming limit curve that was obtained from a limited-scope literature review. Instead, they would be based on a limiting triaxial strain value that is determined from material parameters and equations that are codified in a widely used standard. The downside may be that, as standards are designed to be conservative, the API 579 equations and parameters for aluminium alloys may result in the revised assessments being overly conservative and predicting failures that should not occur. If this is found to be the case, a more tailored approach may be required.

7 Recommendations

In light of the findings of the present work and in conjunction with the detailed discussion about the suitability of the forming limit diagram methodology in its current form, the following recommendations are made:

1. The informative joint design D.14(a) from BS EN 13094:2015, referred to as Generic Banded Type 1 in this report, should be removed from Annex D of the standard, at least in the case of end dishes. This recommendation is based on the following:
 - Tanker Actual Banded Type 1 that is qualitatively similar to this joint design resulted in ruptures at the ends of the flattened portion of the end dish during a full-scale topple test (HSL, 2014).
 - A finite element simulation of a section of tanker Actual Banded Type 1 under topple test conditions and assessed using the forming limit diagram methodology predicted that ruptures would occur in the end dish (TWI, 2015a).
 - Additional finite element analyses undertaken in this report based on a geometry more similar to D.14(a) than Actual Banded Type 1 also predicted that ruptures would occur in the end dish under two material configurations, including one similar to that used in Actual Banded Type 1.
2. Based on the perceived usefulness of the method in quantitatively assessing the mechanical performance and susceptibility of joints to failure, a detailed procedure for performing nonlinear, finite element analysis on a joint design that is made in accordance with Annex D of BS EN 13094 should be

developed and included in BS EN 13094 to be used to assess joint designs that do not conform to those depicted in the informative Annex D, subject to the agreement of the relevant standards-making bodies and the contracting parties to ADR. **This procedure has been developed and is included as Appendix B to this report.**

3. It is envisaged that the methodology and material parameters used in API 579 may be suitable for this, but additional comparison of the API 579 equation with the forming limit diagram used in this report and previous studies should be undertaken to confirm whether this would be appropriate.

8 References

API, 2007: 'API 579-1/ASME FFS-1 Fitness-for-Service', API 579 Second edition, June 5, 2007.

BSI, 2015: 'BS EN 13094:2015 Tanks for the transport of dangerous goods – Metallic tanks with a working pressure not exceeding 0.5bar – Design and Construction', BSI Standards Publication.

DfT, 2014: 'Research specification – Technical Assessment of Petroleum Tankers', DfT Document 140331, Revision 10. 31 March 2014.

HSL, 2014: 'Technical Assessment of Petroleum Road Fuel Tankers Work Package 1 – Full scale testing and associated modelling. Tanker Topple Test Methods and Results', Report ES/14/39/04rev05.

Lakeland, 2004: 'Joint Ring 2', Engineering drawing of extrusion profile design, Document Ref: 77605.

Seipp TG, 2013: 'An Evaluation of the Protection Against Local Failure in ASME Section VIII, Division 2: Finite Element Model Considerations', Proceedings of the 2013 ASME Pressure Vessels and Piping Conference, Volume 3: Design and Analysis, Paris, France, July 14-18, 2013, ISBN: 978-0-7918-5567-6.

SIMULIA, 2014: 'Abaqus Analysis User's Guide', Dassault Systèmes SIMULIA.

TWI, 2014: 'Tanker Testing and Analysis: Work Package 2 Ref: PPRO 04/03/7', TWI Proposal PR23024-2, January 2014.

TWI, 2015a: 'Tanker Testing and Analysis: Work Package 2 Extensions', TWI Proposal No: PR25351-3, 10 July 2015.

TWI, 2015b: 'Department for Transport Technical Assessment of Petroleum Tankers: Metallographic and Analytical Assessment of AT11-1475', TWI Report 24000/13/15, 04 September 2015.

TWI, 2015c: 'Department for Transport Technical Assessment of Petroleum Tankers: Work Package 2 – Detailed Engineering Critical Assessment', TWI Report 24000/9/15, 09 October 2015.

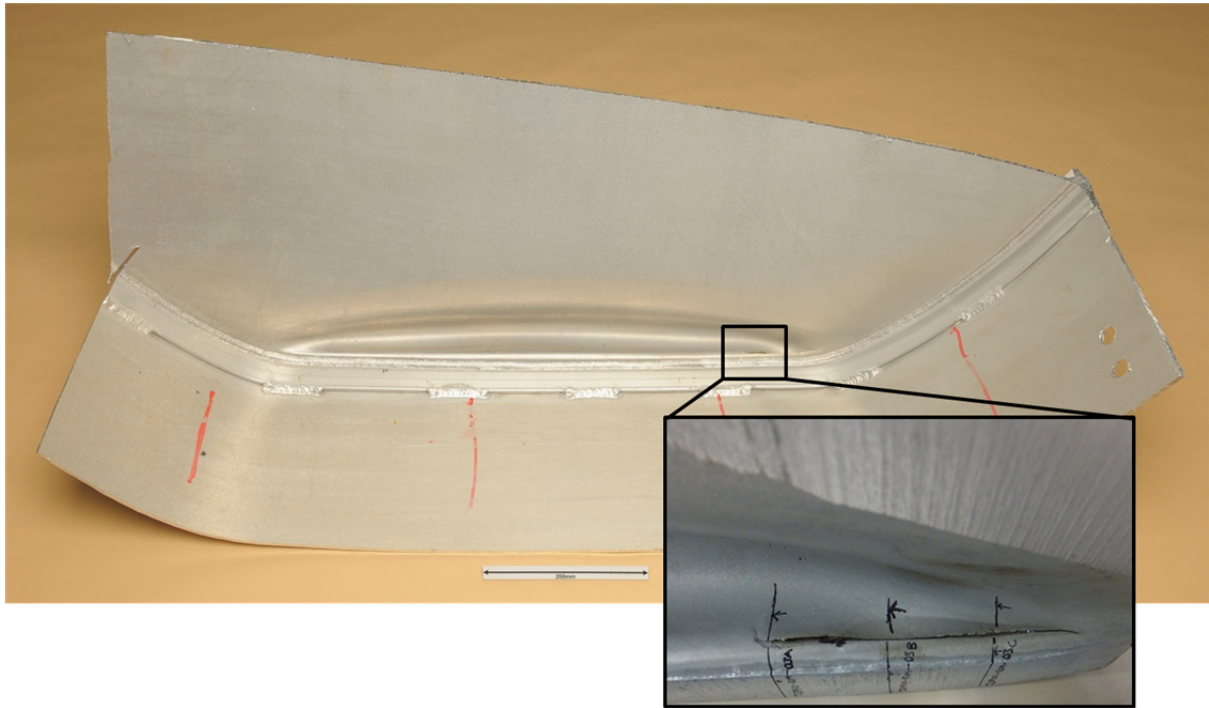


Figure 1 Image of the ruptures that were observed at the ends of the flattened portion of the rear dish of Actual Banded Type 1 after the tople test. Only one side of ruptures shown.

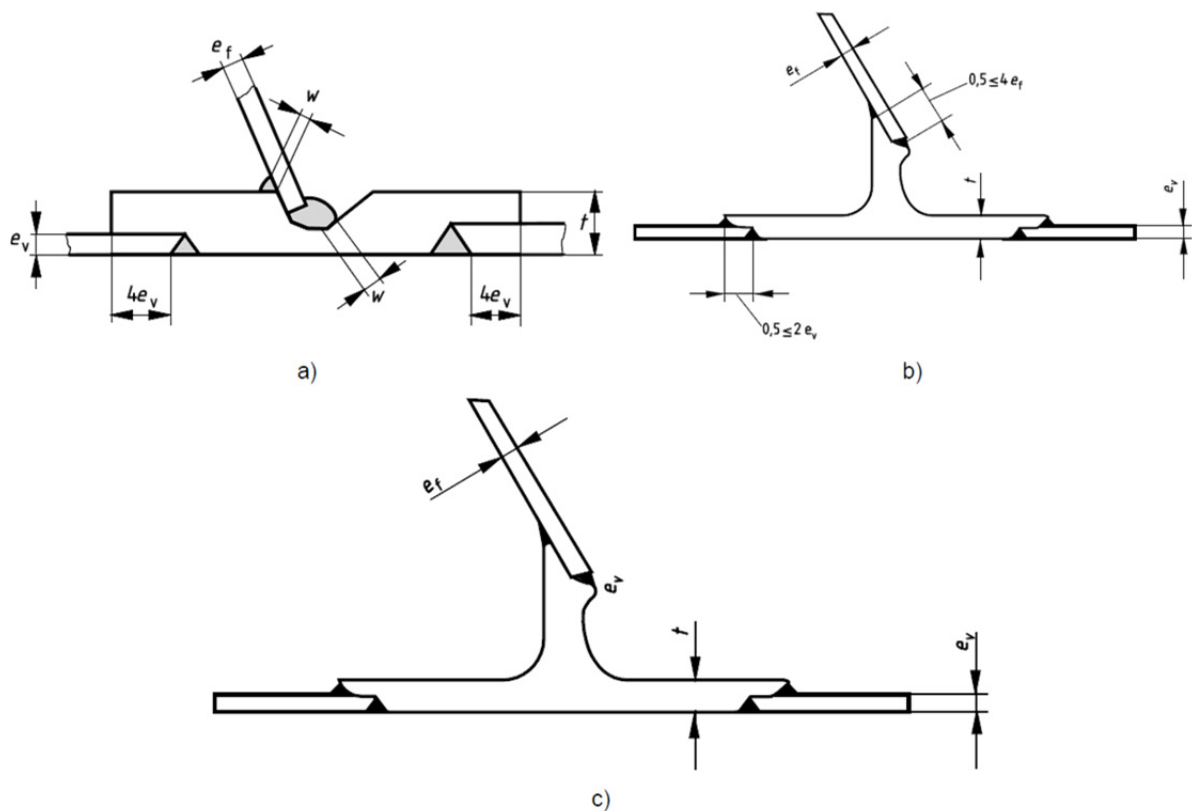


Figure D.14 — Typical partition joints

Figure 2 Figure D.14 (a-c) from BS EN 13094:2015 showing the basis of the Generic Banded Type 1 design in the top left, and the Generic Banded Type 2 design in the top right and bottom centre.

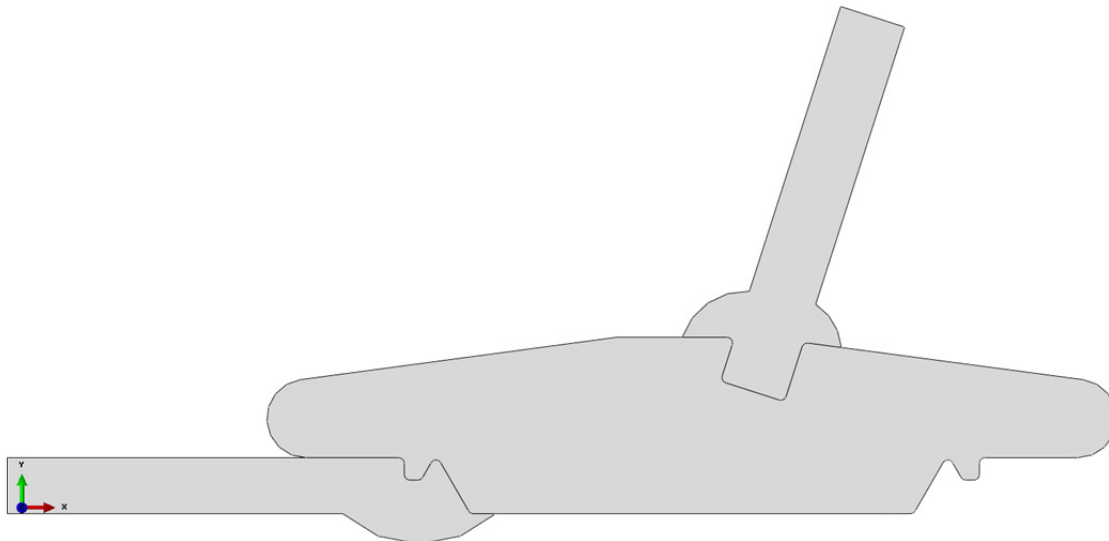
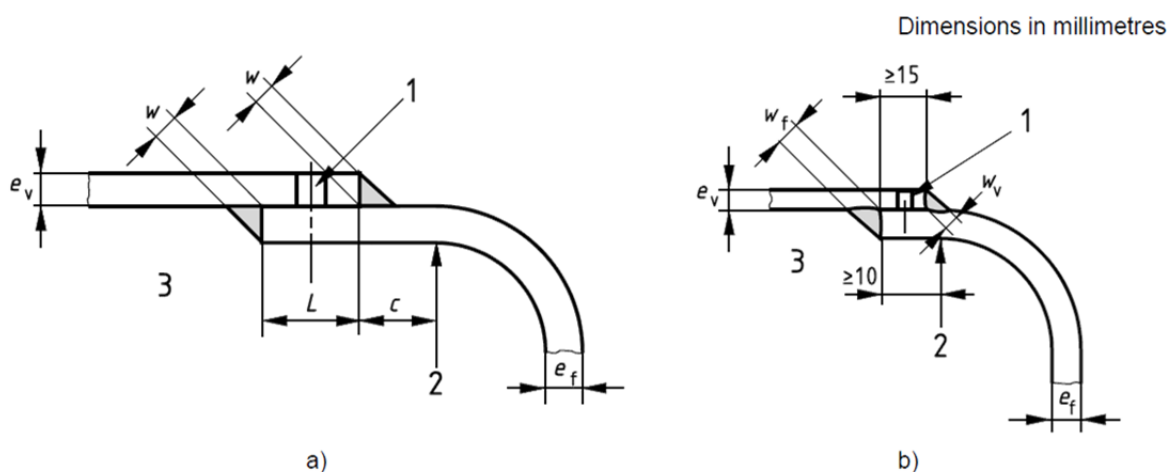


Figure 3 Illustration of the extrusion band geometry for Actual Banded Type 1 that is qualitatively similar to the Generic Banded Type 1 design shown in Figure 1 and analysed in this report.



- Key**
- $c \geq 2 e_v$
 - $e_v \leq 8 \text{ mm}$ $w_v \geq 0,7 e_v$
 - $e_f \leq 8 \text{ mm}$ $w_f \geq 0,7 e_v$
 - 1 tell-tale hole
 - 2 start of radius
 - 3 inside of tank

Figure D.7 — Typical lap joints of an end to a shell

Figure 4 Figure D.7(a-b) from BS EN 13094:2015 showing the basis of the Generic Stuffed Design considered in this report.

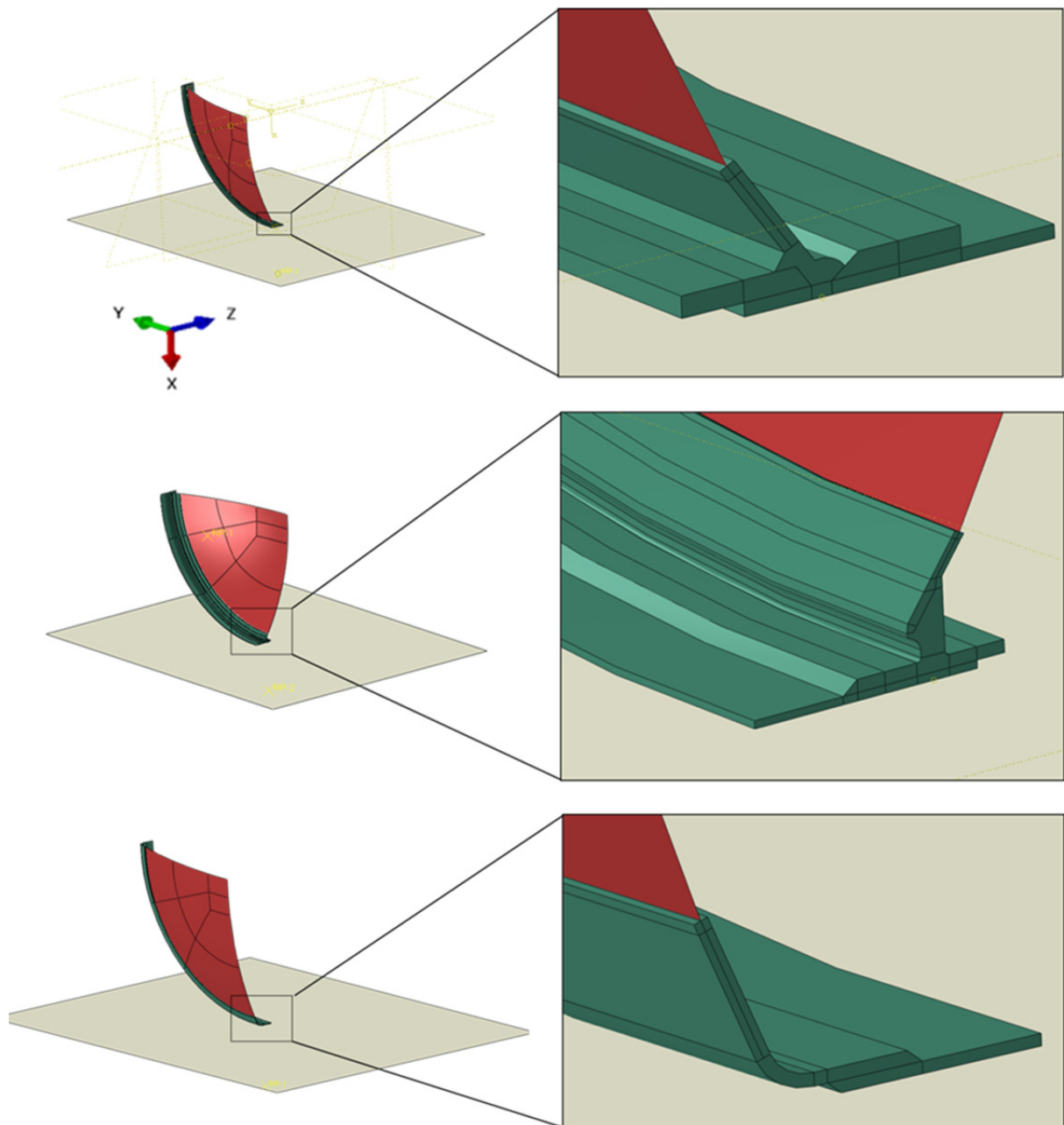
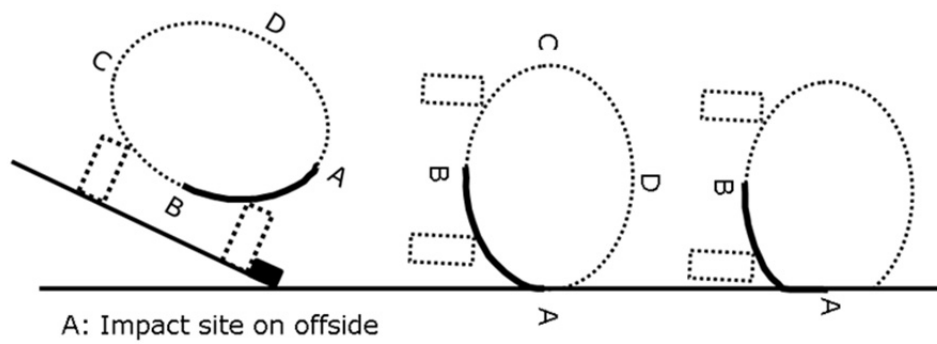


Figure 5 Geometries of the finite element models showing diagram of the topple test in the first row; the Generic Banded Type 1 in the second row; Generic Banded Type 2 in the third row, and Generic Stuffed Design in the bottom row. In all models, the red region is comprised of shell elements and the green regions are comprised of solid, continuum elements.

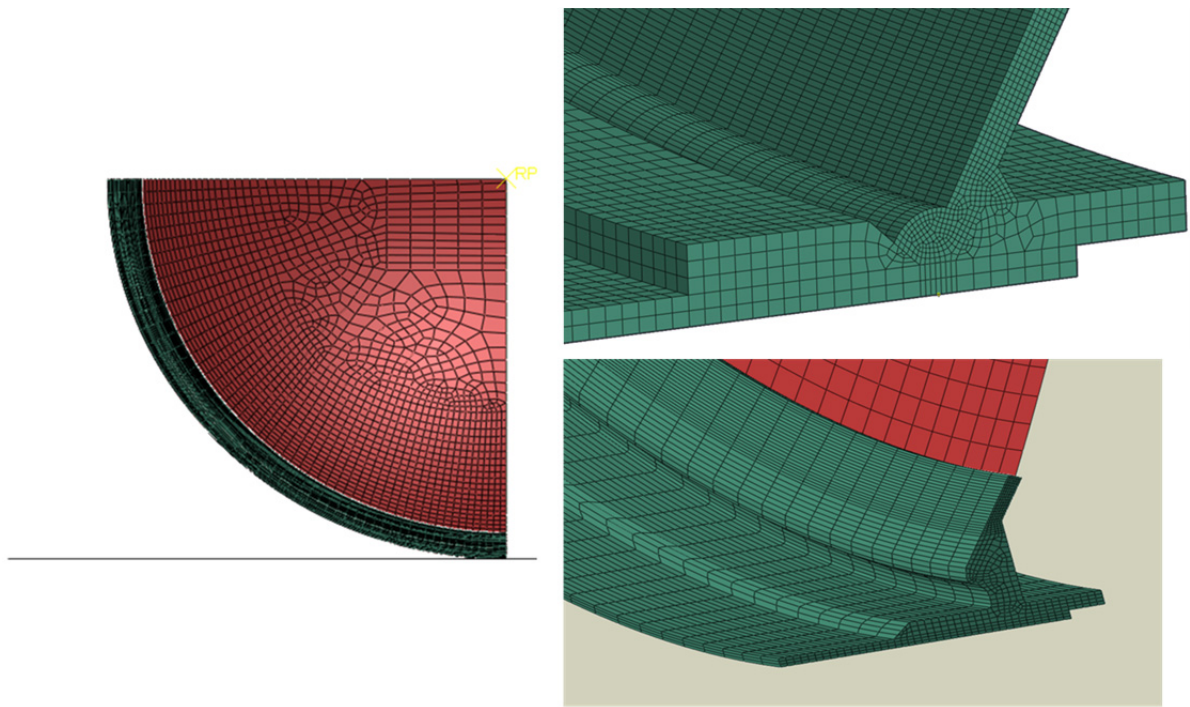


Figure 6 Images of the finite element mesh for Generic Banded Type 1 (top right frame, one material model shown) and Generic Banded Type 2 (bottom right frame, two material model shown). The meshing of the global geometry is shown on the left.

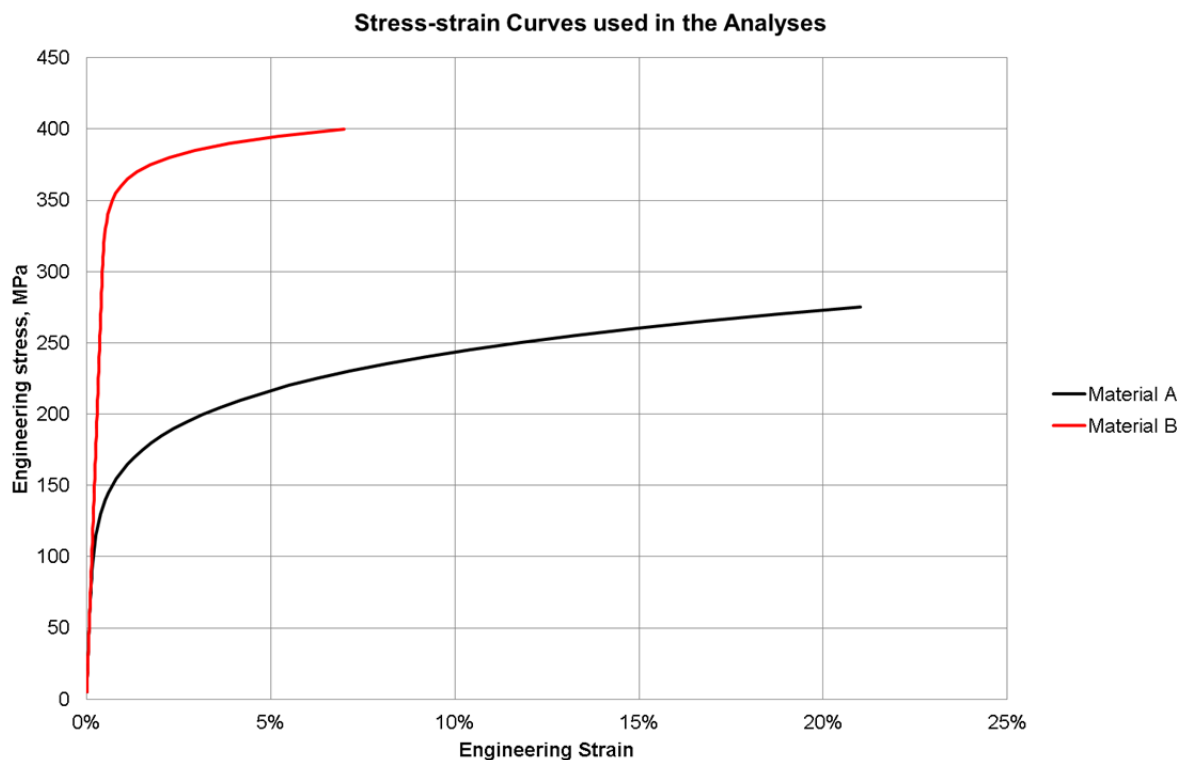


Figure 7 Ramberg-Osgood stress-strain curves derived from the tensile properties of Material A and Material B.

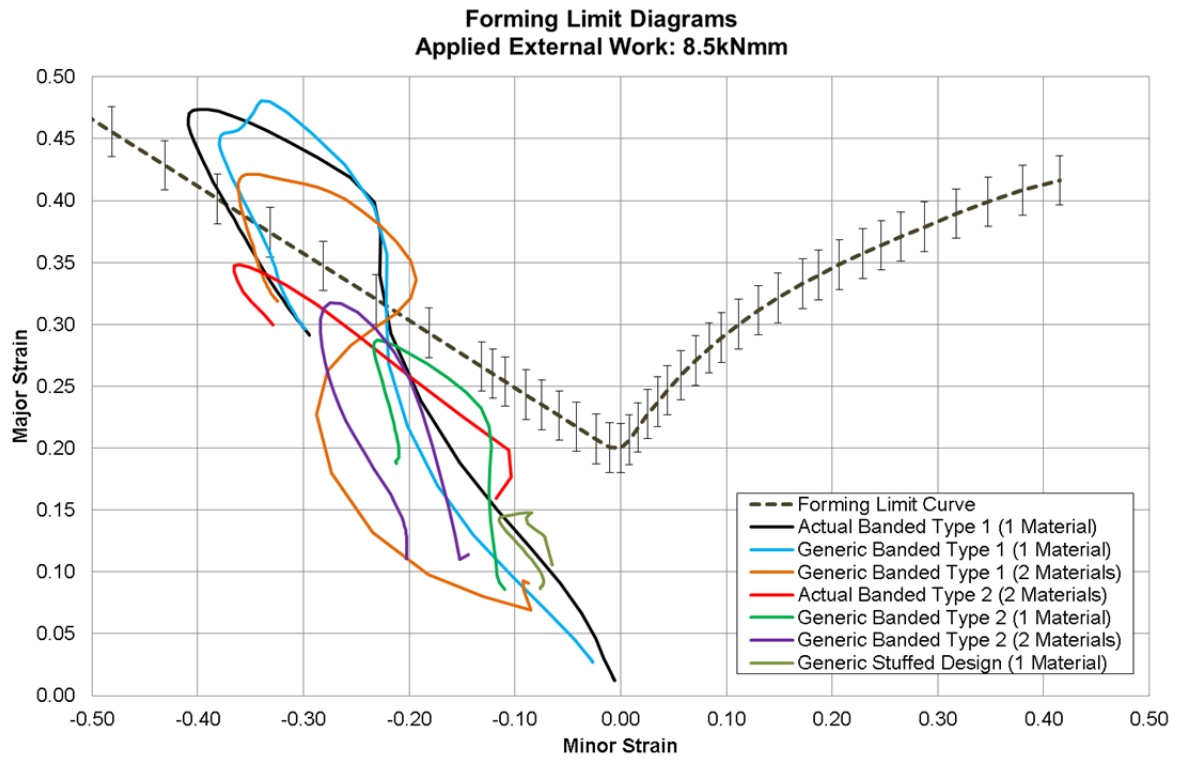


Figure 8 Forming limit diagram for all of the tanker geometries assessed.

Appendix A

Dimensions for the End Joint Design Geometries

Tank Design	Geometry component	Dimension (label and requirements)	BS EN 13094 Diagram / Drawing	Indicative dimension from Actual Banded Type 1 tank	Indicative dimension from Actual Banded Type 2 tank
All	Tanker barrel (cylindrical) shell thickness	$e_v \leq 8.0\text{mm}$	D.7(a-b) and D.14(a-c)	$e_v = 5.0\text{-}5.5\text{mm}$ as measured from macrographs.	$e_v = 5.0\text{-}5.5\text{mm}$ as measured from macrographs.
All	End dish plate thickness	$e_f \leq 8.0\text{mm}$	D.7(a-b) and D.14(a-c)	$e_f = 5.0\text{-}6.0\text{mm}$ as measured from macrographs.	$e_f = 5.0\text{-}6.0\text{mm}$ as measured from macrographs.
All	Weld throat thickness (all)	$w_v \geq 0.7e_v$ $w_f \geq 0.7e_v$	D.7(a-b) and D.14(a)	$5\text{mm} \leq w \leq 7\text{mm}$	$5\text{mm} \leq w \leq 7\text{mm}$ (banded) $4\text{mm} \leq w \leq 6\text{mm}$ (stuffed)
Stuffed	Distance from internal circumferential fillet weld root to external circumferential fillet weld root	$L \geq 15\text{mm}$	D.7(a-b)	N/A	25mm
Stuffed	Distance from the root of the external circumferential fillet weld to the start of the radius of the end dish	$c \geq 2e_v$	D.7(a-b)	N/A	0mm
Stuffed	Radius of the end dish joint	See '2'	D.7(a-b)	N/A	17mm
Banded	Total thickness of the partition joint including the thickness of the tanker shell	$t \geq 8\text{mm}$	D.14(a-c)	$t \geq 12.0\text{mm}$	$t = 13.0\text{mm}$
Banded	Length of overlap between tanker shell and extrusion ring (<u>no additional internal fillet weld</u>)	$4e_v$	D.14(a)	$\sim 7.0\text{mm}$ ($< 4e_v$)	$\sim 7.0\text{mm}$ ($< 4e_v$)
Banded	Length of overlap between tanker shell and extrusion ring (<u>additional internal fillet weld present</u>)	$0.5 \leq 2e_v$	D.14(b)	$\sim 15.0\text{mm}$ (measuring weld centre line to weld centre line)	$\sim 15.0\text{mm}$ (measuring weld centre line to weld centre line)

All	Cross-sectional shape of the tank compartment (oval)	N/A	N/A	Horizontal span (dish): 2525mm Vertical span (dish): 2015mm	Horizontal span (dish): 2467mm Vertical span (dish): 1933mm
All	Dome of rear dish with respect to plane of dish rim	N/A	N/A	250mm	230mm
Banded	Span between centre lines of external circumferential welds	-	D.14 (modified)	~50mm	50mm
Banded	Specific dimensions of profile geometry	Radius of upstand, height of upstand, etc	D.14(b-c)	Specified from engineering drawings	Specified from engineering drawings
Comments	<p>The cross-section of the compartment will be idealised to be an ellipse as opposed to the actual ovalised shape comprised of multiple curvatures used in the Actual Banded Type 1 and Actual Banded Type 2 tanks.</p> <p>The circumferential weld caps for the banded tank design will be assumed to be less than or equal to 1.0mm.</p> <p>All fillet welds will assume equal length legs (ie 45° weld face)</p>				

Appendix B

Numerical Assessment of End Dish to Shell Joints Under Topple Test Conditions

B1 General

This annex describes a general analytical procedure for assessing the designs of tanker end dish to shell joints that do not conform to those depicted in the informative Annex D. The procedure has been validated against experimental measurements obtained from three full-scale topple tests covering three distinct tanker designs and undertaken as part of the UK Department for Transport technical assessment of petroleum road fuel tankers. Full details of topple test setup and the subsequent numerical analyses can be found in the UK Department for Transport reports (HSL, 2014 and TWI, 2015a-b). This annex is divided into five sections which cover:

- B2. Terms, Definitions, Symbols and Abbreviations
- B3. Overview of the Simulation
- B4. Finite Element Analysis Requirements
- B5. Assessment Procedure
- B6. References

B2 Terms, Definitions, Symbols and Abbreviations

B2.1 Terms and definitions

Finite sliding contact

A general contact formulation that allows for the modelling of the interaction between a deformable body and an arbitrarily shaped rigid body where separation and sliding of finite amplitude and arbitrary rotation of the surfaces may arise.

Finite strain theory

In continuum mechanics, the finite strain theory – also called large strain theory, or large (finite) deformation theory – deals with deformations in which both rotations and strains are arbitrarily large and invalidate the assumptions inherent in infinitesimal strain theory. In FEA, this is considered by undertaking a geometrically nonlinear analysis.

First- and second-order elements

First-order elements provide linear interpolation of displacements in the finite element method; second-order elements provide quadratic interpolation of displacements.

Forming Limit Curve (FLC)

See Forming Limit Diagram.

Forming Limit Diagram (FLD)

A Forming Limit Diagram is a graphical representation of material failure due to different states of strain. The FLD has abscissa minor strain and ordinate major strain. The strain plane is separated by the Forming Limit Curve (FLC). The region above the FLC represents a strain state where failure is likely to occur and the region below the FLC represents a strain state where failure is unlikely to occur.

Hybrid element

Hybrid elements treat the pressure stress as an independently interpolated basic solution variable, coupled to the displacement solution through the constitutive theory and the compatibility formulation. They improve accuracy when the material response near-incompressible.

Incremental plasticity theory

Also known as flow theory, is a continuum mechanics theory that is used to describe the plastic (inelastic) behaviour of materials.

Limiting triaxial strain

The limiting triaxial strain is a local failure criteria that is based on the concept of a local strain limit based on the triaxial state of stress. If the equivalent plastic strain at a material point exceeds the limiting triaxial strain, then local failure is likely to occur.

Poisson's ratio

Is the ratio of transverse contraction strain to longitudinal extension strain in the direction of stretching force. Tensile deformation is considered positive and compressive deformation is considered negative. The Poisson's ratio is represented by the Greek letter nu, ν . The Poisson's ratio is dimensionless.

Young's modulus

Also known as the tensile or elastic modulus, is a mechanical property of linear elastic solid bodies that defines the relationship between stress and strain. The Young's modulus is represented by the Latin letter E. Units of the Young's modulus are N/mm^2 (MPa).

B2.2 Symbols and abbreviations

Table 1 Symbols and abbreviations and their definitions.

ϵ_{maj}	Major strain (ie the largest principal strain)
ϵ_{min}	Minor strain (ie the smallest principal strain)
FE	Finite element
FEA	Finite element analysis
FLD	Forming Limit Diagram
FLC	Forming Limit Curve
MPa	Megapascal ($1\text{e}6$ Pa)
mm	Millimetre (unit of Length)
N	Newton (unit of Force)

B3 Overview of the Simulation

The topple test designed by HSL (2014) involves tilting a tanker that has been filled with water under controlled conditions until it becomes unstable and falls onto the offside under gravity alone (Figure B1). A Finite Element (FE) representation of the test uses a static simulation with two planes of symmetry (Figure B1) to analyse the 'crushing' of a three-dimensional cross-section of the tanker between two rigid plates. Previous work (TWI, 2015a-b) found that this simplification of the real topple test can accurately predict the global and local deformation of the tank.

Large strains are experienced under the topple test conditions and the objective of the simulation is to determine the likelihood of rupture in the vicinity of an end joint by comparison with the formability limit of the materials local to the joint. This annex describes a general assessment procedure, or workflow, for performing such an analysis, which involves:

- Generating a FE model based on the tank geometry.
- Specifying the material properties for different regions of the model.

- Calculating the stresses and strains in the FE model from the applied loads and prescribed boundary conditions that represent a static idealisation of the experimental topple test, and
- Analysing the criticality of the stresses and strains using a forming limit diagram (FLD), or an appropriate substitute.

The assessment considers ductile failure only, and therefore it is assumed that all welds have been made to good standards of workmanship and are free of defects such as fabrication flaws (eg lack of side wall fusion).

B4 Finite Element Analysis Requirements

B4.1 Software selection

The computer software used for finite element analysis shall, in addition to the requirements outlined in Annex A.3.1 'Software selection' shall:

- be capable of analysing solid continuum elements;
- be capable of calculating elastic-plastic stresses and strains based on non-linear strain formulation and incremental plasticity theory;
- be capable of implementing contact behaviour between deformable bodies;
- have the ability to average and extrapolate stresses and strains to particular locations within the body under consideration.

B4.2 Validation and reporting

In addition to the requirements of Annex A.3.2 'Validation', both the finite element model and associated input and output files shall be maintained. Specific reporting requirements to ensure that the numerical models can be verified as described in Section B.5.

B5 Assessment Procedure

B5.1 Geometry

B5.1.1 General

The finite element model shall be comprised of at least two distinct parts: the metallic tank and ground.

B5.1.2 Tank geometry

The geometry of the tank shall be generated from relevant manufacturer engineering drawings and diagrams. It is recommended that the local detail of the joint is generated as a solid, three-dimensional component (or assembly of three-dimensional components), but, baffles, end dishes, bulkheads and/or the tanker shell could be analysed using shell theory, provided that the correct stiffness is predicted in these regions (see B5.2.2). The local detail of joints, including the weld throat (and weld profile) dimensions are important, as these details may have a significant effect on the strain concentrations that arise from the large bending moments exerted on the bulkheads during the simulated topple test conditions.

Previous analyses employed quarter-symmetry as shown in Figures B1 and B2 to reduce the computational run-time. Additionally, only the end dish and a fixed axial length of tank shell were modelled. It is recommended that the amount of tank shell modelled is greater than five times the nominal tanker shell wall thickness. The analyst may choose to model more than a single compartment.

B5.1.3 Ground geometry

Due to the large difference between the elastic stiffness of the tank and the ground, it is both appropriate and computationally-efficient to model the ground as a flat, rigid (non-deformable) body. Most commercial FE software has the capability to model rigid bodies either as analytic rigid surfaces or as meshed domains, using code-specific discrete, rigid-element-based surfaces. The analyst may choose to model the ground as a deformable body (or set of deformable bodies) more representative of the conditions previously modelled by HSL (2014).

B5.1.4 Reporting

Reporting of the geometry shall include:

- A description, including images, of the global and local geometry included in the finite element model.
- References to appropriate engineering drawings, diagrams, or images of the physical parts under consideration.
- Descriptions of any geometric simplifications (eg details omitted, simplified weld profiles or regions where dimension reduction has been included), and
- Tables or annotated images detailing the dimensions of all components in the model (eg wall thicknesses, curvatures, and cross-sectional distances).
- Justification as to how the ground has been modelled, whether as a non-deformable or a deformable body (or set of bodies).

B5.2 Finite element mesh

B5.2.1 General

Second-order isoparametric elements are recommended, both in the brick meshing near joints and in the adjacent shell mesh. First order elements can be used, but, it is then important to ensure that the chosen element type and mesh refinement are adequate. Finite strain theory may be needed and the modelling requires contact prediction, so linear elements can provide improved convergence.

There is usually a selection of element integration options available, and some codes have the option of hybrid or reduced integration elements. These elements, in particular, may avoid numerical difficulties associated with the incompressible material behaviour at the fully plastic limit. Benchmark analyses using different options may provide guidance.

B5.2.2 Dimensional reduction

Reports TWI, 2015a-b describe work that successfully employed a dimensional reduction technique to improve computational run times. The entire tanker shell, extrusion bands (when present), circumferential welds and a short annular section of the end dish was made with solid, continuum elements. The rest of the end dish was then modelled with continuum shell elements with a suitable coupling along the interface between the shell elements and solid elements for the displacements (and rotations) of the shell element nodes onto the adjacent solid element nodes. Dimensional reduction techniques can be employed in the finite element model provided the local geometry is appropriate for such a procedure to be applied.

B5.2.3 Reporting

Reporting of the finite element mesh shall include:

- A description of the element types employed.
- A description of the characteristic element sizes, and
- Images of the finite element mesh that show regions of local mesh refinements and regions of the different element types (if present). If different element types are included, a description of the coupling along all incompatible element interfaces shall be provided.

Mesh sensitivity studies should be undertaken to demonstrate that the modelling method is suitable. The results of mesh sensitivity results should be reported.

B5.3 Material Properties

B5.3.1 General

Rate-independent, isotropic hardening, von Mises yield and an associated flow rule has been successfully used to simulate previous topple tests and to predict the onset of tearing using a FLD (TWI, 2015a-b). This material model is therefore recommended.

All material properties shall be specified at -20°C (or at the minimum design temperature where this is lower).

B5.3.2 Elastic properties

The required elastic properties are the Young's modulus, E , and the Poisson's ratio, ν .

B5.3.3 Non-linear properties

The stress-strain curve for the material should be defined up to the maximum expected predicted strains. If values beyond the defined range are encountered, the finite element code will adopt a default procedure based on the data provided, but this may not be correct.

Finite element codes will generally require the stress-strain curve to be defined as a series of discrete data points (multi-linear, incremental plasticity theory), the minimum requirement being one or two data points.

The stress-strain relationship shall be defined as either engineering stress against engineering strain or, alternatively, true stress against the logarithm of plastic strain. It is important that this definition is made correctly with respect to the FE code being used, particularly for the topple test conditions where large strains and finite deformation theory is required.

B5.3.4 Reporting

Reporting of material properties shall include:

- A description of all materials data that are used in the simulation including the source (literature, material specification or test data), uncertainties and the units of material data.
- Any assumed material properties shall be accompanied by a justification of the assumed values.
- The material model employed in the simulation.
- Graphical or tabular representations of the stress-strain curves for the materials included in the simulation, and
- Figures of the locations of different materials in the finite element model.

B5.4 Prescribed Conditions and Interactions

B5.4.1 General

The applied loads and prescribed boundary conditions have been designed to represent the complex forces exerted on the tank by both the contained fluid and the ground during the topple test.

B5.4.2 Applied loads

A pressure of 0.2MPa (2bar) shall be applied to all internal surfaces of the tank. This pressure represents the pressure impulse that the contained fluid exerts on the inner surface of the tank during impact (HSL, 2014). In the static analysis (see B5.5), the pressure shall ramp from zero at the start of the simulation to 0.2MPa at the final solution increment. The effect of gravity and self-weight can be included, but have been found to have only a negligible influence on the solution.

B5.4.3 Prescribed boundary conditions

The analyst shall specify the global coordinate system and any local coordinate systems that have been used to define the boundary conditions. For the purposes of this annex, the boundary conditions are specified independent of any specific coordinate system and are instead defined as follows with respect to the labelling convention in Figures B1 and B2:

- All nodes along the cross section represented by line BF and the curve BG are restrained in the AC direction. The plane passing through points B, F and G is assumed to be a symmetry plane passing through the top and bottom of the tank along the entire length of the tank.
- All nodes along the cross section represented by the line AE and the curve AG are restrained in the BD direction. The plane passing through points A, E and G is assumed to be a symmetry plane during the analysis.
- Rotation of the model edges on the two planes should also be restrained. This may require an explicit boundary condition if shell elements are being used anywhere on these edges.
- All nodes along the cross section represented by the curve EF are restrained in the AE direction (ie in the axial direction of the tank). This represented a pseudo-symmetry plane mid-compartment.
- All displacements, except the vertical displacement, of the 'ground' shall be constrained.

For a quarter symmetry model, the magnitude of the ground displacement into the tank shall be defined as follows:

- Let L be defined as the axial component of the distance from G to E (see Figure B2).
- Let $W(d_i)$ be the energy dissipated through plastic deformation (plastic dissipation) plus the elastic strain energy, and the energy dissipated through friction after a ground displacement, d_i (see Figure B2).
- The total ground displacement for the simulation, d_{total} , shall be equal to the ground displacement increment at which $W(d_{total}) = (30644.2N)L$. In this equation, the units of length shall be millimetre (mm) and the unit of work (or energy) is Nmm.

This definition was obtained by validating previous FE models against experimental measurements from three full-scale topple tests. If quarter symmetry is not employed, then the energy value shall be scaled appropriately.

For example, if symmetry about the AC plane is included, then the energy value shall be double.

B5.4.4 Contact formulation

A finite sliding (or equivalent) contact definition shall be defined between all external surfaces and the computational domain representing the ground. Additionally, a self-contact definition for all external surfaces of the tank shall be defined. The contact definition shall be selected as appropriate to minimise the penetration of the tank element nodes into the computational domain representing the ground. The friction between the contacting bodies can be included with the isotropic Coulomb friction model, using a tangential friction coefficient between 0.1 and 0.3. The results are relatively insensitive to the magnitude of the friction coefficient, but a sensitivity analysis may be required if self-contact becomes extensive.

B5.4.5 Reporting

Reporting of the loads and boundary conditions shall include:

- A description of the global (and local, if appropriate) coordinate systems in which the loads and boundary conditions have been specified.
- Annotated figures of the finite element model showing the locations of prescribed loads and boundary conditions.
- A description of the contact algorithm and associated contact parameters included in the model, and
- A description, including annotated figures if appropriate, of distributed couplings used in the finite element model.

B5.5 Analysis Procedure

B5.5.1 General

It is recommended that a static, implicit analysis procedure that incorporates large strains and the finite deformation theory is employed, whereby the inertial effects are neglected. This type of analysis procedure was used in the simulations that provided the framework for this annex (TWI, 2015b).

It may be difficult to obtain solution convergence with a static, implicit solver due to strong nonlinearities arising from the finite strain formulation, mesh design, nonlinear material properties and contact algorithms. This can be overcome by use of an implicit, dynamics solver in which inertial effects are introduced primarily to reduce the overall level of the unstable behaviour. However, considerable numerical dissipation may occur and sensitivity of the results with respect to the solution increment size should be analysed.

B5.5.2 Reporting

Reporting of the analysis procedure shall include:

- A description of the analysis procedure (eg the type of solver).
- A description of the finite element analysis solver (including the version).

B5.6 Analysis of Results

B5.6.1 General

All simulations set up in accordance to the guidelines of this annex shall be appropriately verified.

The likelihood of rupture in the vicinity of joints in the shell may be determined using either a forming limit diagram approach (see Sections B5.6.2 and B5.6.3) or a limiting triaxial strain approach (B5.6.4). The assessments described in these sections are to be undertaken at the solution increment corresponding to the total ground displacement described in Section B5.4.3.

B5.6.2 Assessment by forming limit curve for EN AW-5182

A forming limit diagram (FLD) provides a graphical description of ductile material failure under a range of biaxial loading conditions. The material is likely to fail when the condition of applied strain is above the forming limit curve (FLC) defined as a locus of points with x-coordinate minor strain and y-coordinate major strain. A literature review of forming limit curves for EN AW-5182, the aluminium alloy of the bulkheads and tanker shells previously analysed, was undertaken to provide a lower bound estimate of an appropriate forming limit diagram (Wu et al, 2003; Abedararabbo et al, 2005; Soare et al, 2008; and Li et al, 2011) and is given below in Equation B.1 and shown in Figure B3:

$$\epsilon_{\text{maj}} = \begin{cases} -0.54\epsilon_{\text{min}} + 0.20 & \text{if } \epsilon_{\text{min}} < 0 \\ 2.6906\epsilon_{\text{min}}^3 - 2.6198\epsilon_{\text{min}}^2 + 1.1519\epsilon_{\text{min}} + 0.20 & \text{if } \epsilon_{\text{min}} \geq 0 \end{cases} \quad [\text{B.1}]$$

Where:

ϵ_{maj} is the major strain (or maximum principal strain) in mm/mm.

ϵ_{min} is the minor strain (or minimum principal strain) in mm/mm.

The analyst shall identify whether there are positions in the model where the resulting strain state is above the forming limit curve. Care is needed to assess whether the strain derivation method (including extrapolation method, perhaps to the surface nodes of the model) is accurate.

B5.6.3 Assessment by forming limit curve for other metals

The forming limit diagram methodology described in Section B5.6.2 may be modified for use with other metals, provided appropriate material data is found and the source, reliability and suitability of an alternative forming limit curve is documented and recorded.

B5.6.4 Assessment by limiting triaxial strain for other metals

The forming limit curve in Equation B.1 for EN AW-5182 was based on published literature rather than the specific testing of material under appropriate conditions of, for example, strain-rate, test temperature and specimen thickness. For other materials, a more generic procedure can be used that is based on the concept of a limiting triaxial strain. In such a method, the maximum sustainable equivalent failure strain is determined as a function of stress triaxiality. At any position in the model where the equivalent plastic strain exceeds the position-specific, triaxiality-dependent failure strain, then local failure is deemed to occur. A widely adopted limiting triaxial strain method is detailed by Seipp (2013), including material parameters suitable for stainless steel, ferritic steels and aluminium alloys.

B5.7 Sensitivity study

The safety of the proposed assessment method is, in part, determined by the accuracy of the assumed mechanical properties. Reliable test data is important,

however, it is likely that some form of approximation will be made. These shall be thoroughly documented, but, in addition, a sensitivity study is recommended to determine if the likely level of assumption could be of importance to the level of predicted safety.

B6 **References**

Abedarabbo N, Pourboghrat F and Carsely JE, 2005: 'Forming of EN AW-5182 and AA5754-O at elevated temperatures using coupled thermo-mechanical finite element models', *International Journal of Plasticity*, Volume 23, Issue 5, May 2007, pp 841-875, ISSN 0749-6419.

BSI, 2015: BS EN 13094:2015 'Tanks for the transport of dangerous goods – Metallic tanks with a working pressure not exceeding 0.5bar – Design and construction', British Standards Institution, 2015.

HSL, 2014: 'Technical Assessment of Petroleum Road Fuel Tankers Work Package 1 – Full scale testing and associated modelling. Tanker Topple Test Methods and Results', Report ES/14/39/04rev05.

Li J, Hu S, Carsley JE, Lee TM, Hector LG, Jr and Mishra S, 2011: 'Postanneal Mechanical Properties of Restrained EN AW-5182-O Sheets', *Journal of Manufacturing Science and Engineering*, Volume 133, Issue 6, doi: 10.1115/1.4004613

Seipp TG, 2013: 'An Evaluation of the Protection Against Local Failure in ASME Section VIII, Division 2: Finite Element Model Considerations', *Proceedings of the 2013 ASME Pressure Vessels and Piping Conference*, Volume 3: Design and Analysis, Paris, France, July 14-18, 2013, ISBN: 978-0-7918-5567-6.

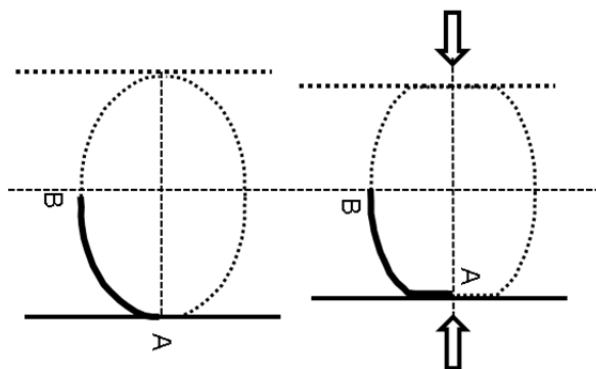
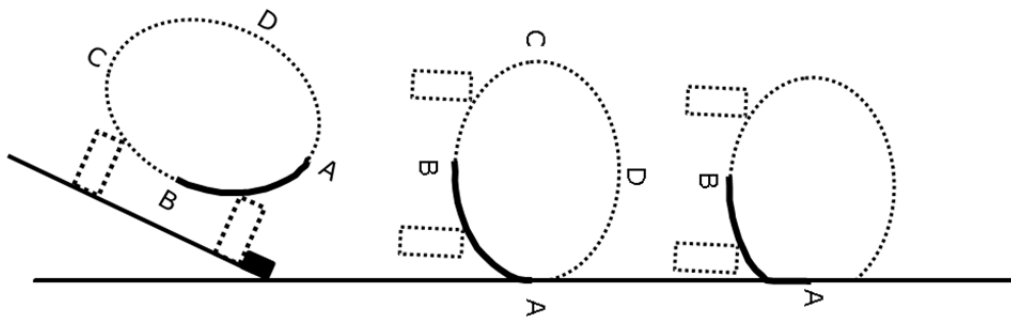
Soare S, Yoon JW and Cazacu O, 2008: 'On the use of homogeneous polynomials to develop anisotropic yield functions with applications to sheet forming', *International Journal of Plasticity*, Volume 24, Issue 6, June 2008, pp 915-944, ISSN 0749-6419.

TWI, 2015a: TWI Report 24000/13/15 'Department for Transport Technical Assessment of Petroleum Tankers: Metallographic and Analytical Assessment of AT11-1475', 4 September 2015.

TWI, 2015b: TWI Report 24000/9/15 'Department for Transport Technical Assessment of Petroleum Tankers: Work Package 2 – Detailed Engineering Critical Assessment', 9 October 2015.

Wu PD, Jain M, Savoie J, MacEwen SR, Tuđcu P and Neale KW, 2003: 'Evaluation of anisotropic yield functions for aluminum sheets', *International Journal of Plasticity*, Volume 19, Issue 1, January 2003, pp 121-138, ISSN 0749-6419.

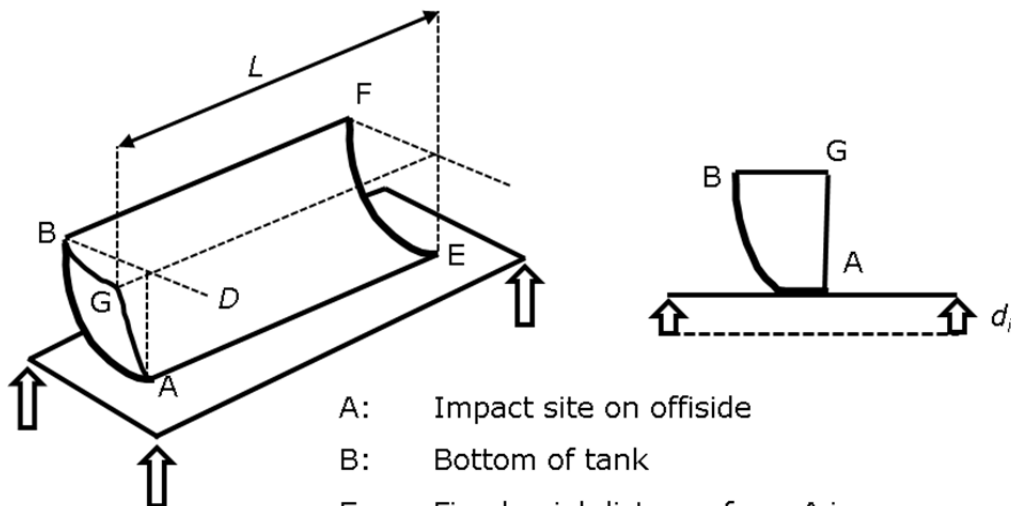
Experimental topple test conditions



A: Impact site on offside
 B: Bottom of the tank
 C: Nearside, opposite A
 D: Top of the tank

Simulated topple test conditions

Figure B1 Illustration of the experimental topple test conditions (top three figures) compared to the simulated topple test conditions (bottom two figures). Line AB (shown in bold) is analysed in the model and the dashed straight lines (bottom) indicated assumed planes of symmetry.



A: Impact site on offside
 B: Bottom of tank
 E: Fixed axial distance from A in same compartment
 F: Fixed axial distance from B in same compartment
 G: Apex of the domed end dish

Figure B2 Illustration of the three-dimensional simulated topple test geometry. One quarter of the end dish is represented by the dome quadrant traced out by the curve ABGA. The labels L and d_i are those corresponding to the variables used to determine the crushing displacement.

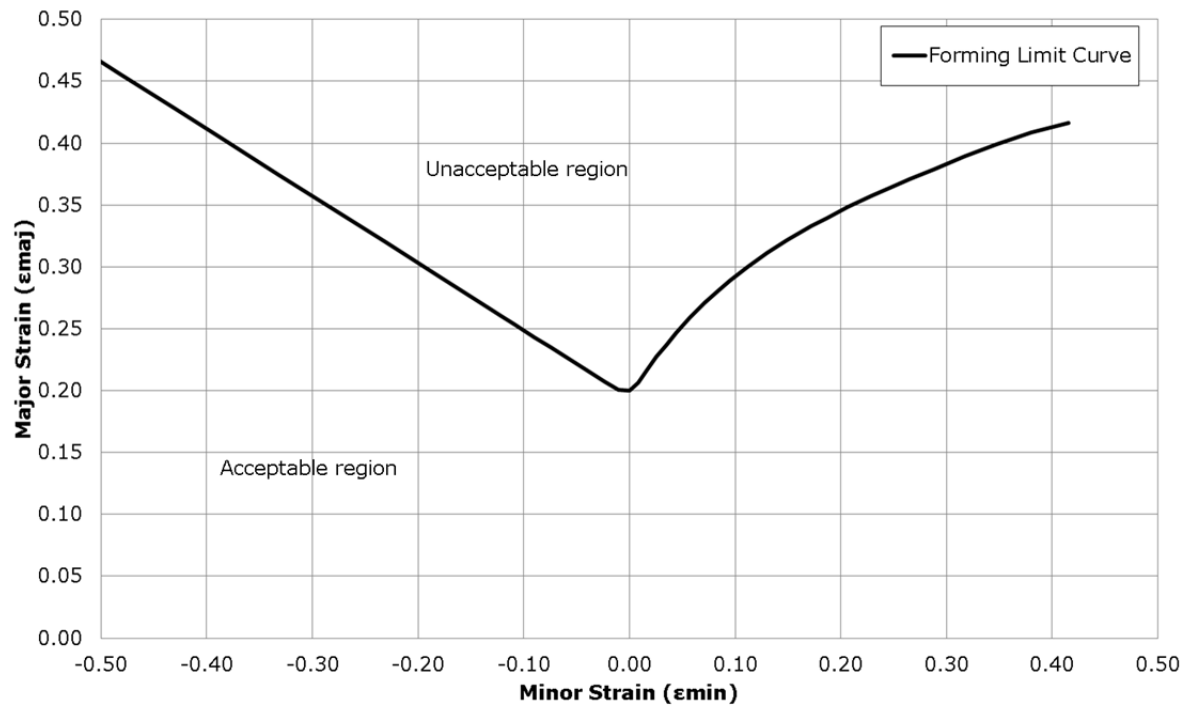


Figure B3 Example of a forming limit diagram using the forming limit curve from Equation B.1.

TWI Management System

TWI operates a Management System designed to ensure that customer requirements are met and that any work carried out is conducted in a planned and controlled manner. Customer satisfaction is a key measure of the success of TWI, which remains committed to delivering world-class solutions. To this end:

- All technical activities are controlled by a management system that complies with the general requirements of the BS EN ISO 9000:2008 series of standards.
- Project management, examination and training services are audited by LRQA as complying with BS EN ISO 9001:2008 and software development in accordance with TickITplus, Certification Number 0925004.
- TWI is a UKAS accredited testing laboratory No. 0088. Specific details are given on the UKAS Schedule of Accreditation, available at www.ukas.org. Reports may contain information not included in the TWI schedule of accredited tests. Enquiries concerning accreditation of tests should be directed to the Quality and Safety Group.
- Examination activities are assessed by PCN to BINDT requirements and by TWI Certification Ltd to CSWIP requirements.
- TWI is certificated by LRQA to BS EN ISO 14001:2004, certificate number LRQA 4000756.
- TWI's Occupational Health and Safety Management System is certificated to BS OHSAS 18001:2007 by LRQA, certificate number 4004571.

The Management System operated by TWI includes the following features that are particularly relevant to ensuring the success of projects:

- Close and frequent contact with the customer is requested of the Project Leader throughout the project. In particular, changes in personnel involved in the project or equipment availability are discussed together with any project delays or contractual changes.
- Regular management reviews of projects are held throughout the life of a project and upon its completion. These cover finance, technical progress and adherence to schedule.
- Project sponsors are formally contacted on project completion by senior TWI management to determine their satisfaction with the work carried out. Moreover, TWI management welcomes feedback on project progress at all times during the course of the work. Significant lapses in service are subjected to a structured management review so that inadequate procedures are identified and improved.



TWI Ltd
Granta Park, Great Abington
Cambridge CB21 6AL
United Kingdom

Tel: +44 (0)1223 899000
Fax: +44 (0)1223 892588
Web: www.twi-global.com

VAT Number GB 700 1708 89

Registered Number 3859442 England